Pearlite in multicomponent steels: phenomenological steady-state modeling

Jiayi Yan, John Ågren, Johan Jeppsson
Thermo-Calc Software AB, Sweden
Presented by: Kaisheng Wu, Thermo-Calc Software Inc., USA

TMS 2020
26 Feb 2020, San Diego, USA

Outline

- Austenite-to-pearlite transformation
  - Assumptions for modeling
- Steady-state growth rate: driving-force–dissipation balance
  - Finite interfacial mobility
  - Constrained carbon equilibrium and “optimal pearlite”
  - Solute drag
- Grain boundary nucleation rate
  - Effect of grain boundary segregation
- Summary

The austenite-to-pearlite transformation and assumptions for modeling

- Cooperative eutectoid transformation
- Continuous lamellar composite in spherical colonies
  - Divorced (degenerate) or rod microstructure not considered
- Constant (steady-state) growth rate and lamellar spacing
  - Divergent pearlite (due to soft impingement) not considered

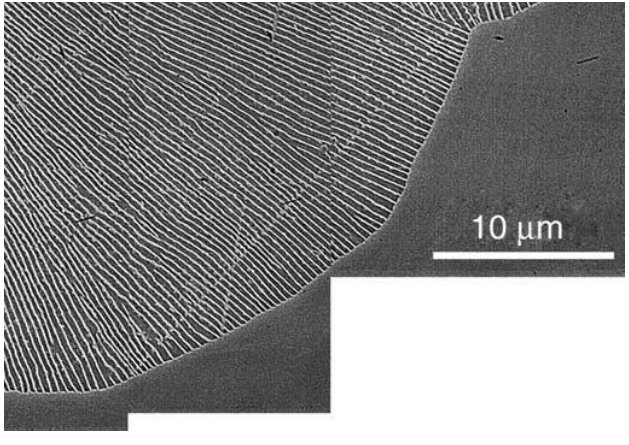

Fe–2.46C–3.50Mn (at.%)
5h at 625°C (α+θ two-phase region)
C.R. Hutchinson, R.E. Hackenberg, and G.J. Shiflet: Acta Mater., 2004, vol. 52, pp. 3565–85.

Steady-state growth rate: a driving-force–dissipation balance approach

$$G_m^{\gamma} - \left[(1-f^{\theta})G_m^{\alpha} + f^{\theta}G_m^{\theta}\right] = \frac{2\sigma V_m}{S} + \frac{v}{M^I} + (1-f^{\theta})\sum_{j=1}^{m}\Delta G_{m,j}^{SD} + \frac{vS(f^{\theta})^2}{2}\sum_{i=1}^{n}\frac{(u_i^0-u_i^{\theta})^2}{u_i^0\left[M_i^{\gamma}+\frac{2(kM^{B\|}\delta)_i}{S}\right]}$$

Driving force ΔG_m
γ→α+θ
TCFE database

Formation of α/θ interface

Interfacial friction γ/P

Solute drag on γ/α interface

Volume and boundary diffusion (in parallel)

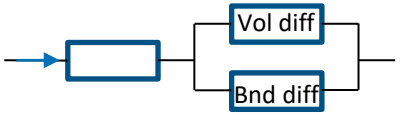

- This equation defines v as a function of S
- Driving force depends on α and θ compositions (to be revisited)

Comparison to previous modeling approaches

- Previous models all have advantages and simplifications for different model ingredients. In comparison, we have …
- Simplified capillarity consideration
  - Not considering equilibrium of surface tension at γ/α/θ trijunction
- Simplified volume diffusion field
  - Not looking for local equilibrium at γ/α or γ/θ interface
- Added finite interfacial mobility and solute drag

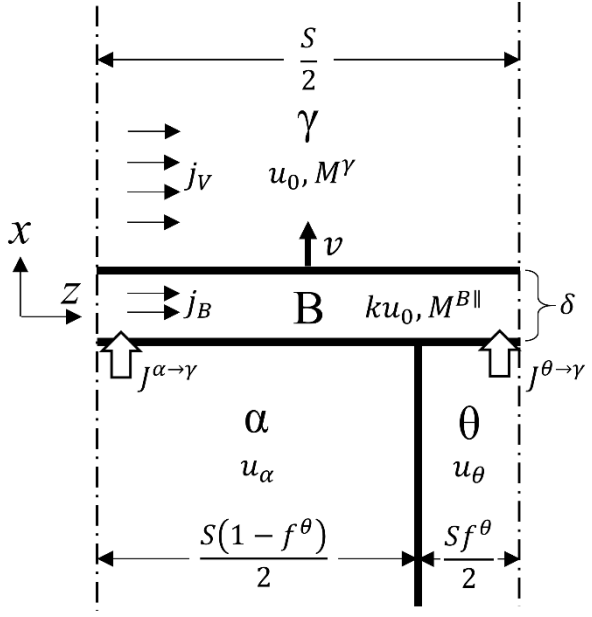

Significance of finite interfacial mobility

- Critical spacing: $S_c = 2\sigma V_m / \Delta G_m$, where $v = 0$
- Can obtain unique v and S by $\mathrm{d}v/\mathrm{d}S = 0$
- For infinite interfacial mobility, $S/S_c = \cdots$
  - 2 for volume-diffusion control
  - 1.5 for boundary-diffusion control
  - 1.5~2 for mixed control
- Finite interfacial mobility allows $S/S_c > 2$
  - Previously $\sigma^{\alpha/\theta}$ >1J/m² (too high) for S to agree with experimental value
  - With finite M^I, $\sigma^{\alpha/\theta}$ can be 0.5J/m² (reasonable)

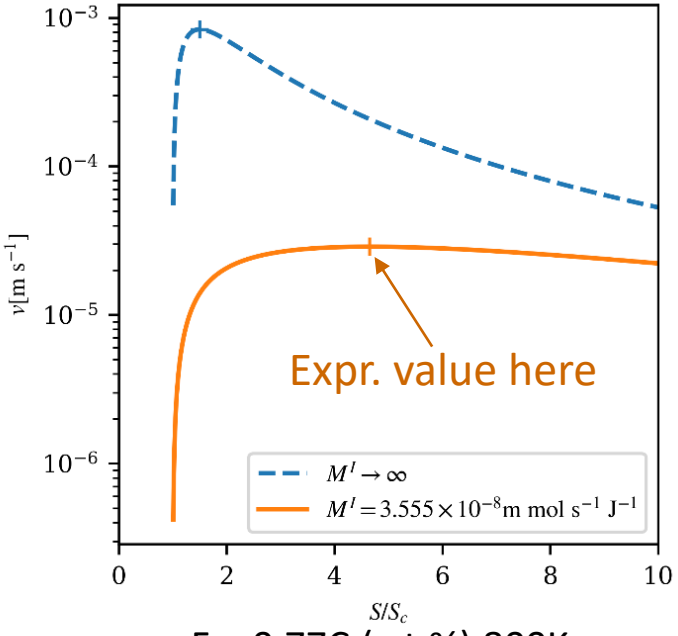

Fe–0.77C (wt.%) 800K

σ=0.5J/m², fixed $\left(kM^{B\|}\delta\right)_C$

Temperature dependence of interfacial mobility

- Non-Arrhenius temperature dependence of interfacial mobility
  - First discovered in 1976*
  - Parameterized empirically in this work
  - Can possibly be modeled based on ledge mechanism of growth as observed** (future work)

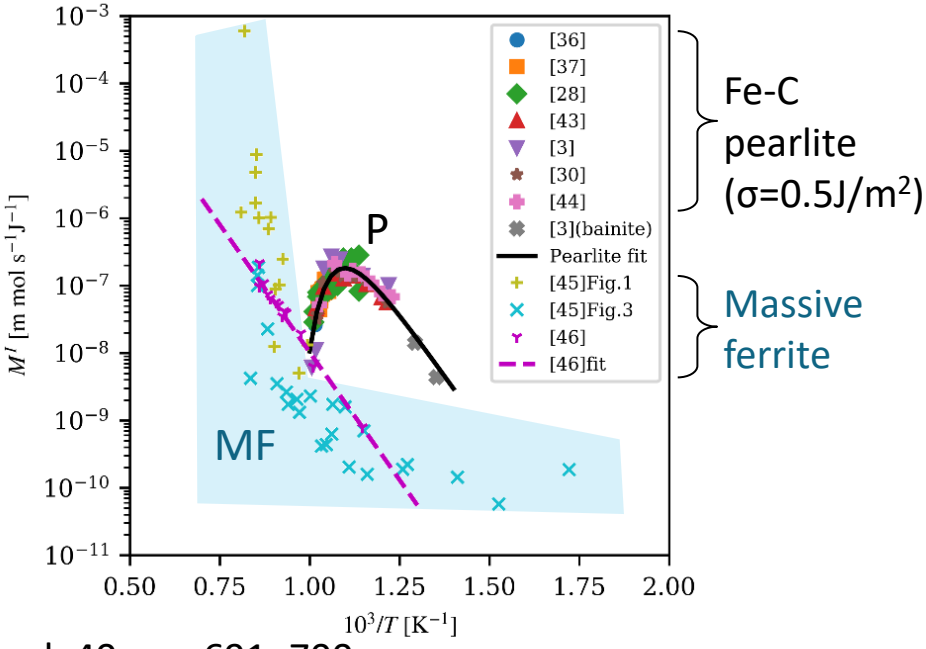

*F. Togashi and T. Nishizawa: J. Japan Inst. Met., 1976, vol. 40, pp. 691–700

**For example, D.S. Zhou and G.J. Shiflet: Metall. Trans. A, 1991, vol. 22A, pp. 1349–65

Constrained Carbon Equilibrium (CCE)

- In alloyed steel, driving force (and then growth rate) depends on the θ:α partition coefficient(s) $K_i^{\theta/\alpha}$ of substitutional alloying elements
  - $K_i^{\theta/\alpha}$ from orthoequilibrium (OE): orthopearlite, usually at high T
  - $K_i^{\theta/\alpha} = 1$ (paraequilibrium, PE): parapearlite, usually at low temperature
- In general they are two special cases of CCE under an arbitrary $K_i^{\theta/\alpha}$

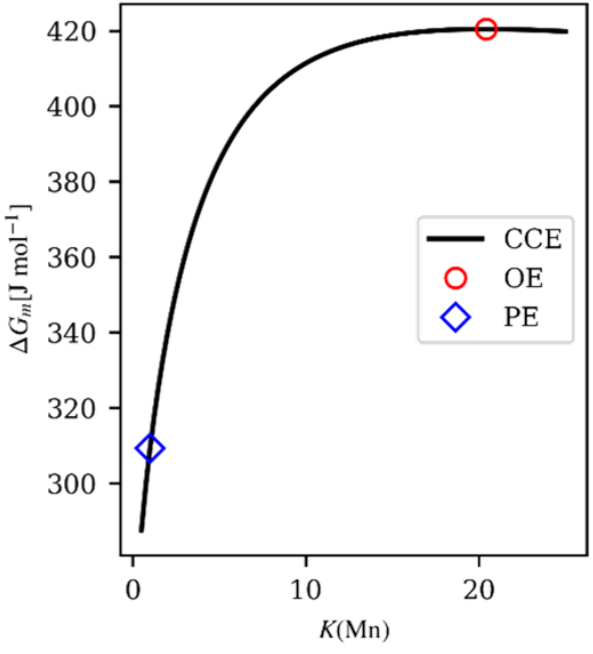

Fe–0.69C–1.80Mn (wt.%) T=900K

Thermo-Calc Software

“Optimal pearlite”

- Can maximize v wrt S and $K_i^{\theta/\alpha}$: “optimal pearlite”

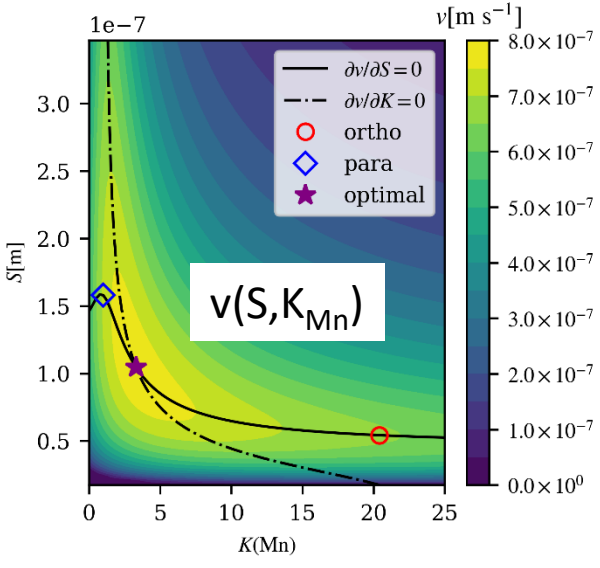

Fe–0.69C–1.80Mn (wt.%) T=900K

- Can realize a smooth transition from orthopearlite to parapearlite from high-T to low-T

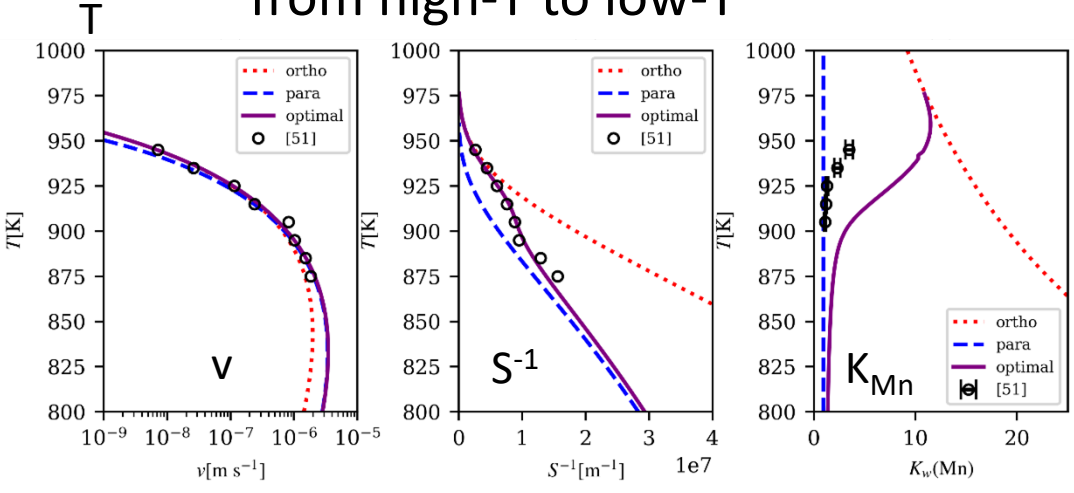

Fe–0.69C–1.80Mn (wt.%)

Dissipation mechanisms

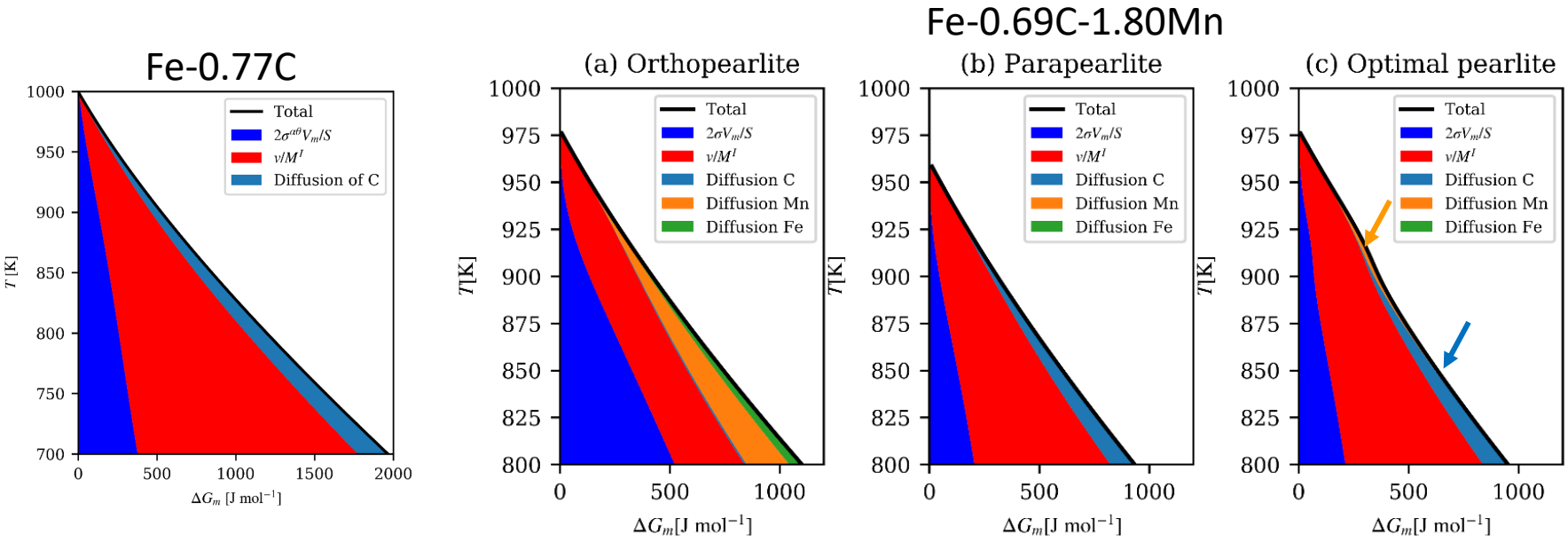

- Interface- and diffusion-mixed control (even for Fe-C)
- Element generating most dissipation by diffusion: M for orthopearlite, C for parapearlite, M→C for optimal pearlite

Solute drag

- Using Cahn's model (1962) for simplicity

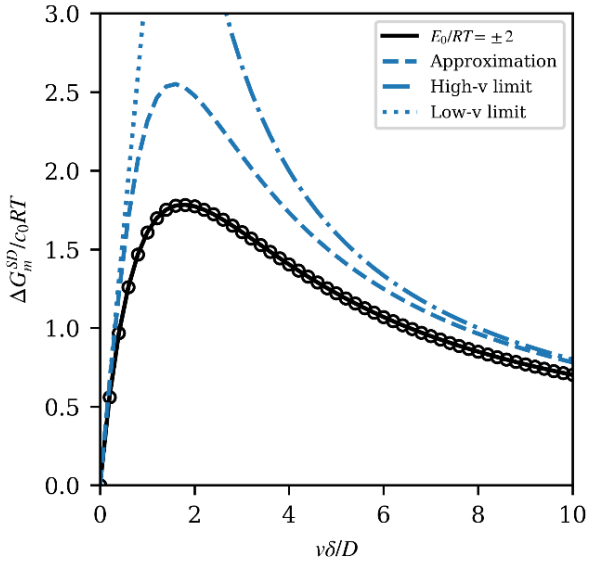

- Can describe the "bays" on growth curves for Cr- and Mo-containing alloys

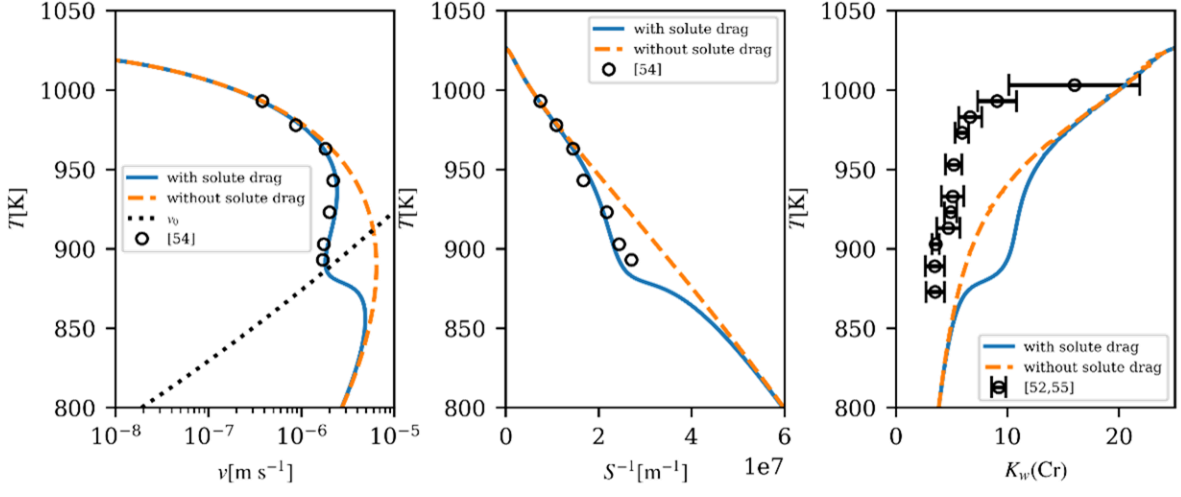

Fe–0.6C–1.78Cr (wt.%)
Optimal pearlite

Nucleation rate and overall transformation kinetics

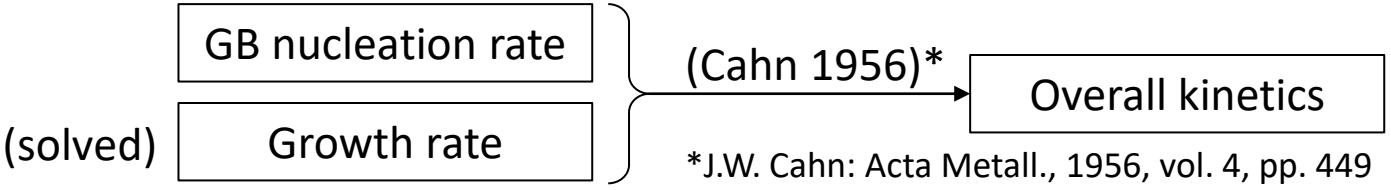

*J.W. Cahn: Acta Metall., 1956, vol. 4, pp. 449

- GB nucleation rate is modeled and fitted to overall kinetics
  - Time-independent GB nucleation rate is enough to describe overall kinetics
  - Direct measurement of GB nucleation rate is scarce but shows time dependence (not understood physically!)

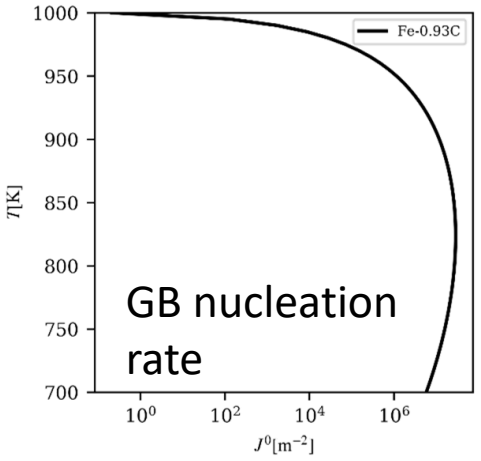

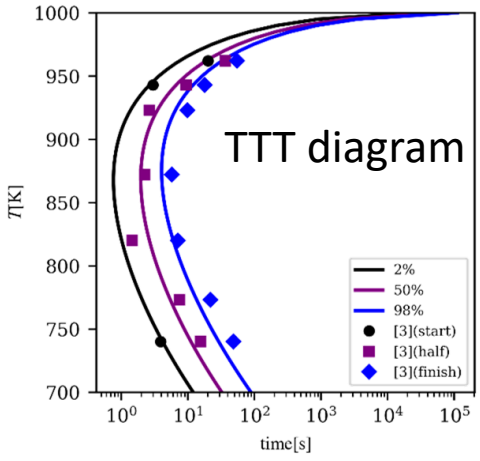

Fe-0.93C (wt.%)

Grain boundary segregation and nucleation rate

- GB nucleation rate should depend on GB concentration
- GB concentration modeled by equilibrium McLean isotherm

$$u_i^{GB} = u_i^0 \exp\left(\frac{E_i^{GB}}{RT}\right)$$

- Can describe the dramatically retarded transformation below the nose for Cr-steels

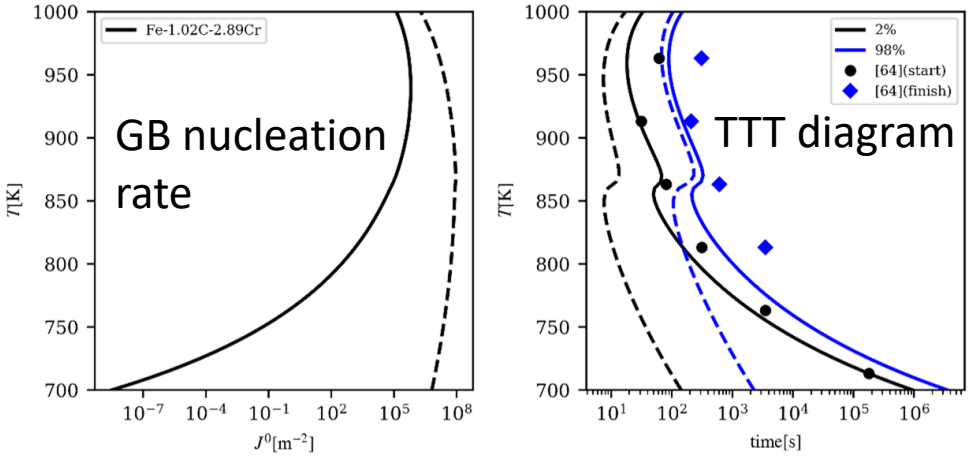

Fe-1.02C-2.89Cr (wt.%)
Dashed curves: without GB segregation
Solid curves: with GB segregation

Summary

- Steady-state modeling of pearlite growth and nucleation
  - Suitable for multicomponent steel using CALPHAD databases
- Finite interfacial mobility and solute drag are introduced for growth
- “Optimal pearlite”: Partitioning of substitutional elements in pearlite can be optimized, which realizes an ortho-para transition
- GB nucleation rate (with effect of GB segregation) and overall kinetics are modeled

J.-Y. Yan, J. Ågren, J. Jeppsson, Metall Mater Trans A (2020), accepted
Notes after presentation: Paper published in Vol. 51A pp. 1978-2001

Thermo-Calc implementation

- Pearlite Property Model in Thermo-Calc since Version 2019a

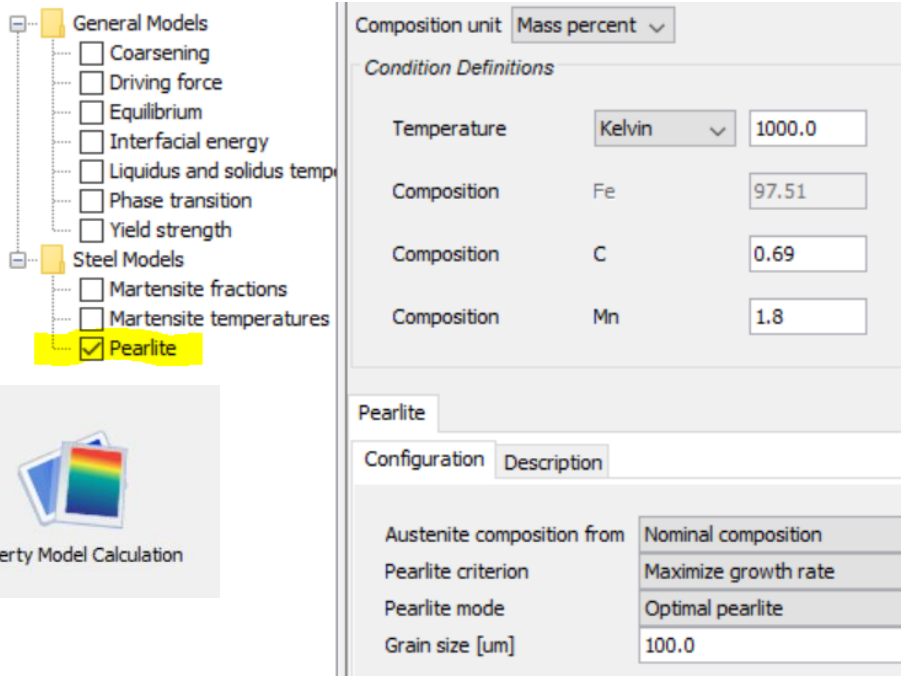

Example
PM_Fe_03

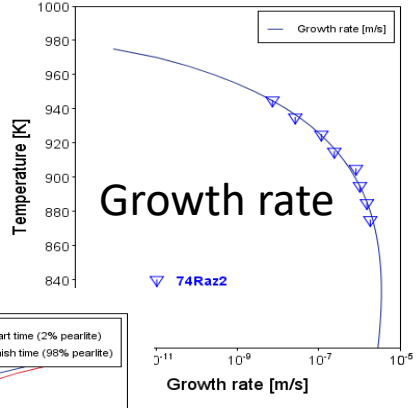

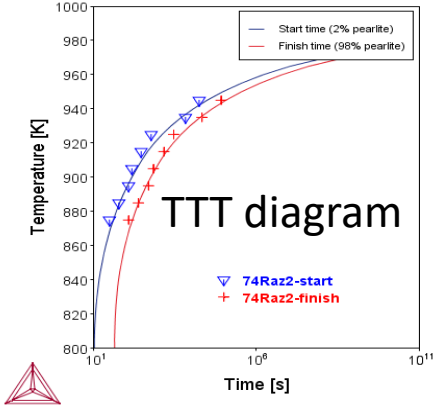

Including Fe, C, Mn, Cr, Mo, W, Si, Al, Ni, Co